SEGMENTATION OF TIBIA BONE IN ULTRASOUND IMAGES USING ACTIVE SHAPE MODELS

Ping He, Jun Zheng

Department of Biomedical, Industrial and Human Factors Engineering
Wright State University, Dayton, Ohio 45435, USA

Abstract – **This paper describes the use of Active Shape Models to segment the tibia bone in ultrasound images. Using CT images from three volunteers, a training set consisting of 60 tibia contours, each represented by 45 labeled points, is first established. After aligning the contours in the training set, a Point Distribution Model (PDM) is generated that includes a mean shape of tibia and six modes of shape variation that explain 98% of the total shape variation. Using the PDM, a new shape can be generated which is further scaled, rotated and translated to match the tibia contour in an ultrasound image. Preliminary results indicate that Active Shape Models provide a useful tool for segmenting leg bones in ultrasound images.**

***Keywords* – Active shape models, segmentation, tibia bone, ultrasound image**

I. INTRODUCTION

Edge detection and structure segmentation for ultrasound images are very challenging processes due to the relatively poor image quality. Traditional automated algorithms often fail in such applications. An example is segmentation of tibia and fibula from ultrasound images obtained by scanning the residual limb of an amputee for the purpose of computer-aided prosthetic socket design [1]. In these images, the shading effect of the bones causes the contours of tibia and fibula to appear "incomplete" in the inner portions where the two bones face each other. In this paper, we report the preliminary results of using "Active Shape Models" (ASMs) [2] to segment tibia from ultrasound images. ASMs use a deformable template generated from a training set to segment the targeted structure from the image. Statistical parameterization provides global shape constrains and allows the model to deform only in ways implied by the training set. We found that ATMs are the suitable choice for segmenting tibia from ultrasound images.

II. METHOD

Implementation of ASMs consists of three steps. The first step is to prepare a training set that includes various possible shapes for the targeted structure (in the current application, it is the contour of tibia cross section). The second step is to generate a Point Distribution Model (PDM) by analyzing the statistics of the set of aligned shapes. The third step is to use the PDM to actually segment the targeted structure in an image. In the following sections, we describe each of the three steps using our specific examples.

A) Prepare a set of aligned training shapes

60 CT images are taken from both legs of three volunteers (two amputees and a healthy person). Contour of tibia in each image is detected and the shape of tibia is represented by a set of 45 labeled landmark points on the contour. To facilitate the alignment of the shapes in the training set, three anchor points are first placed on each contour. The anchor points are generally related to some identifiable anatomical features of the structure. For example, in our current application, the first anchor point is chosen as the point closest to fibula, and the other two define the turning points of the bone contour, as shown in Fig. 1.

Next, 12, 16, and 14 equally-distanced points are placed between the first & second, second & third, and third & first anchor points, respectively. Together with the three anchor points, these 45 landmark points represent a sample of the shape of tibia.

Let us use two vectors, $\mathbf{S}_1$ and $\mathbf{S}_2$, to describe the coordinates of the n (n = 45 in the current application) landmark points of two shapes in the training set:

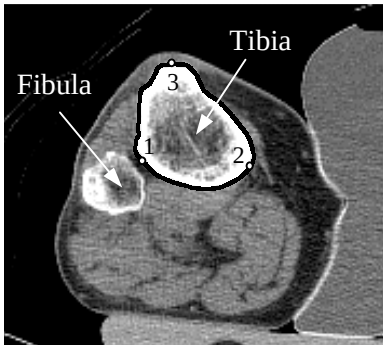

Fig. 1 An example of a CT image of a leg, showing the detected contour of tibia and three anchor points labeled as 1, 2, and 3.

Report Documentation Page

Report Date	Report Type	Dates Covered (from... to)
25 Oct 2001	N/A	-

Title and Subtitle Segmentation of TIBIA Bone in Ultrasound Images Using Active Shape Models	**Contract Number**
	Grant Number
	Program Element Number
Author(s)	**Project Number**
	Task Number
	Work Unit Number
Performing Organization Name(s) and Address(es) Department of Biomedical Industrial and Human Factors Engineering Wright State University Dayton, OH 45435	**Performing Organization Report Number**
Sponsoring/Monitoring Agency Name(s) and Address(es) US Army Research, Development & Standardization Group (UK) PSC 802 Box 15 FPO AE 09499-1500	**Sponsor/Monitor's Acronym(s)**
	Sponsor/Monitor's Report Number(s)

Distribution/Availability Statement
Approved for public release, distribution unlimited

Supplementary Notes
Papers from 23rd Annual International Conference of the IEEE Engineering in Medicine and Biology Society, October 25-28, 2001, held in Istanbul, Turkey. See also ADM001351 for entire conference on cd-rom.

Abstract

Subject Terms

Report Classification unclassified	**Classification of this page** unclassified
Classification of Abstract unclassified	**Limitation of Abstract** UU

Number of Pages
4

$$\mathbf{S}_1 = (x_{11}, y_{11}, \ldots\ldots x_{1k}, y_{1k}\ldots\ldots x_{1n}, y_{1n})^T \quad (1)$$

$$\mathbf{S}_2 = (x_{21}, y_{21}, \ldots\ldots x_{2k}, y_{2k}\ldots\ldots x_{2n}, y_{2n})^T \quad (2)$$

where (x_{1k}, y_{1k}) and (x_{2k}, y_{2k}) are coordinates of the k'th point of shape 1 and shape 2, respectively. The difference between these two shapes can be defined as:

$$d_{12} = (\mathbf{S}_2 - \mathbf{S}_1)^T(\mathbf{S}_2 - \mathbf{S}_1) \quad (3)$$

We may consider that this difference is contributed by two sources. The first source is the pose difference (different size, orientation, and position) between the two shapes, and the second source is the intrinsic shape variation. The first source can be removed by scaling, rotating, and translating the second shape with respect to the first shape in an attempt to minimize d_{12}. The operation of scaling $\mathbf{S}_2$ by a factor s, rotating by an angle θ, and translating by a vector **t** can be described by the following equation:

$$\mathbf{S}_2^* = \mathbf{M}(s, \theta)\mathbf{S}_2 + \mathbf{t} \quad (4)$$

where **M** is a 2×2 matrix:

$$\mathbf{M}(s, \theta) = \begin{pmatrix} s\cos(\theta) & -s\sin(\theta) \\ s\sin(\theta) & s\cos(\theta) \end{pmatrix} \quad (5)$$

and **t** is a translation vector with a length of 2n:

$$\mathbf{t} = (t_x, t_y, t_x, t_y, \ldots\ldots t_x, t_y)^T \quad (6)$$

For a given pair of $\mathbf{S}_1$ and $\mathbf{S}_2$, one can solve for the pose parameters s, θ, and **t** that minimize d_{12} [3]. When d_{12} is minimized, we say the two shapes are aligned, and the remaining difference indicates the intrinsic shape variation between $\mathbf{S}_1$ and $\mathbf{S}_2$.

The above minimization procedure is also applied to $\mathbf{S}_3$, $\mathbf{S}_4$, …. and finally $\mathbf{S}_{60}$ so that the entire training set is aligned.

B) Generate a Point Distribution Model (PDM)

The mean shape, $\bar{\mathbf{S}}$, and the covariance matrix, **C**, of the aligned shapes in the training set are calculated as:

$$\bar{\mathbf{S}} = \frac{1}{N}\sum_{i=1}^{N}\mathbf{S}_i \qquad (\text{N = 60 in this case}) \quad (7)$$

$$\mathbf{C} = \frac{1}{N}\sum_{i=1}^{N}(\mathbf{S}_i - \bar{\mathbf{S}})(\mathbf{S}_i - \bar{\mathbf{S}})^T \quad (8)$$

where $\mathbf{S}_i$ is the vector (with a length of 2n) describing the coordinates of the 45 landmark points of the i'th shape in the aligned training set and **C** is a 2n×2n matrix. Fig. 2 shows the mean shape of the 60 aligned shapes of tibia. The figure also shows the 45 labeled landmark points. The three anchor points now become the 1'st, 14'th, and 31'st landmark points, respectively.

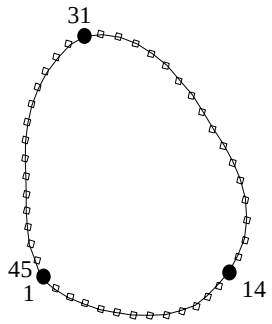

Fig. 2 Mean shape of tibia obtained from 60 aligned training shapes, and 45 landmarks points. The 1st, 14th and 31st points are the original anchor points.

Based on the *principle components analysis*, the modes of variation of the points of the shape are represented by the unit eigenvectors $\mathbf{\Phi}_i$ (i = 1 to 2n) of the covariance matrix **C**:

$$\mathbf{C}\mathbf{\Phi}_i = \lambda_i\mathbf{\Phi}_i \quad (9)$$

where λ_i is the i'th ordered eigenvalue of **C**, $\lambda_i > \lambda_{i+1}$. Since the proportion of the total variance explained by each eigenvector is equal to the corresponding eigenvalue, most of the shape variation can usually be explained by the first few modes. In our case of modeling the shape of tibia, it is found that 98% of the total shape variation in our training set can be explained by the first 6 eigenvectors. As a result, any shape in the training set can be approximated using the mean shape and a weighted sum of the deviations obtained from the first 6 modes:

$$\mathbf{S} \cong \bar{\mathbf{S}} + \mathbf{\Phi}\mathbf{b} \quad (10)$$

where $\mathbf{\Phi} = (\mathbf{\Phi}_1, \mathbf{\Phi}_2, \ldots\mathbf{\Phi}_6)$ is the matrix of the first 6 eigenvectors, and $\mathbf{b} = (b_1, b_2 \ldots b_6)^T$ is a vector of suitable weights for individual eigenvectors.

Equation (10) allows us to generate new examples of the shape by varying the parameters (b_i) within a suitable limit. Since the variance of b_i can be shown to be λ_i, a suitable limit which is used in the current application is:

$$-3\sqrt{\lambda_i} \le b_i \le 3\sqrt{\lambda_i} \quad (11)$$

C) Using PDM to segment the targeted structure

Having generated PDM, we can now search and segment the targeted structure in an image. The overall approach can be summarized as consisting of two steps. Step 1 is to use (10) to generate a suitable seed model shape $\mathbf{S}_0$:

$$\mathbf{S}_0 = \bar{\mathbf{S}} + \mathbf{\Phi}\mathbf{b} \quad (12)$$

Step 2 is to change the pose of $\mathbf{S}_0$ so that the resulted shape **S** best matches the boundary of the targeted structure:

$$\mathbf{S} = \mathbf{M}(s, \theta)\mathbf{S}_0 + \mathbf{t} \quad (13)$$

Since we already have $\bar{\mathbf{S}}$ and $\mathbf{\Phi}$, the task is to determine the shape parameter **b** and the pose parameters s, θ and **t**, for a given image. This is accomplished by using the following iterative procedure.

1) Initialization. Initially, the shape parameter, **b**, is set to zero in (12). Based on a visual inspection of the targeted structure (tibia) in the image, an initial shape **S** is generated to approximate the structure by manually adjusting the pose parameters s, θ, and **t**:

$$\mathbf{S} = \mathbf{M}(s, \theta)\mathbf{S}_0 + \mathbf{t} = \mathbf{M}(s, \theta)\,\bar{\mathbf{S}} + \mathbf{t} \qquad (14)$$

2) Search for the boundary of the targeted structure. From each model point (previously called the landmark point) in **S**, search for the possible edge point of the target along a search line that is perpendicular to the boundary of **S** at that point. Fig. 3 depicts this searching process.

To determine the edge point along the search line, the 1D pixel profile is first smoothed with a 1D Gaussian filter. A derivative operator is then used to compute the gradient magnitude. Finally, the edge point is defined as the point where the gradient magnitude is the largest and is also larger than a predetermined threshold. This edge search is performed locally. In our present study, the search line has 15 pixels on each side of the model point. If, within the search range, there is no edge point that meets the threshold requirement, the original model point is used as the default edge point.

After the above edge searching process is performed for each model point, a displacement vector $\Delta\mathbf{S} = (dx_1, dy_1, \ldots dx_k, dy_k, \ldots dx_n, dy_n)^T$ is produced where (dx_k, dy_k) is the difference vector between the edge point for the k'th model point and the k'th model point. The desired boundary of the structure at this time is represented by the n edge points whose coordinates are represented by vector $\mathbf{Y} = (\mathbf{S} + \Delta\mathbf{S})$.

3) Align the model shape **S** with the current edge **Y**. To align the model shape **S** with **Y,** the pose parameters in (14) have to be further changed (updated) so that the difference between the new shape **S** and **Y** is minimized (this is the same problem as to align $\mathbf{S}_2$ with $\mathbf{S}_1$ discussed earlier):

$$\mathbf{S} = \mathbf{M}(s(1+ds), (\theta+d\theta))\mathbf{S}_0 + (\mathbf{t}+d\mathbf{t}) \qquad (15)$$

where ds, dθ and d**t** are the additional changes in the pose parameters so that the difference between **S** and **Y** is minimized. However, by adjusting the pose parameters along will not perfectly match the model shape with the edge **Y** due the intrinsic difference between the original seed shape $\mathbf{S}_0$ and **Y**. The remaining difference between **S** and **Y** can be removed only by adjusting the original seed shape of the model. In other words, the following transformation produces a model shape which would match the desired structure **Y**:

$$\mathbf{M}(s(1+ds), (\theta+d\theta))(\mathbf{S}_0+d\mathbf{S}) + (\mathbf{t}+d\mathbf{t}) = \mathbf{Y} \qquad (16)$$

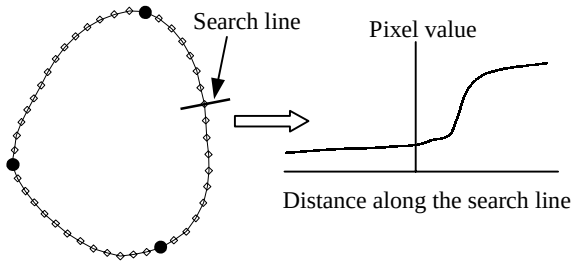

Fig. 3 Left: an initial shape **S** represented by 45 points, showing edge searching for a particular model point. **Right**: possible 1D pixel profile along the search line.

It can be proven that $\mathbf{M}^{-1}(s, \theta) = \mathbf{M}(s^{-1}, -\theta)$. The required adjustment, d**S**, to the seed shape, $\mathbf{S}_0$, can then be found as:

$$d\mathbf{S} = \mathbf{M}(s^{-1}(1+ds)^{-1}, -(\theta+d\theta))(\mathbf{Y}-\mathbf{t}-d\mathbf{t}) - \mathbf{S}_0 \qquad (17)$$

4) Adjust the shape parameter **b**. For the desired change in the seed shape as defined by (17), we wish to find the parameter adjustment d**b** so that:

$$\mathbf{S}_0 + d\mathbf{S} = \bar{\mathbf{S}} + \mathbf{\Phi}\mathbf{b} + d\mathbf{S} \cong \bar{\mathbf{S}} + \mathbf{\Phi}(\mathbf{b}+d\mathbf{b}) \qquad (18)$$

The adjustment d**b** can then be solved as:

$$d\mathbf{b} = \mathbf{\Phi}^T(d\mathbf{S}) = \mathbf{\Phi}^{-1}(d\mathbf{S}) \qquad (19)$$

Finally, the shape parameter is updated by the following equation (with the constraint defined by (11)):

$$\mathbf{b} = \mathbf{b} + d\mathbf{b} \qquad (20)$$

5) Generate a new model shape using the updated seed model shape:

$$\mathbf{S} = \mathbf{M}(s(1+ds), (\theta+d\theta))(\bar{\mathbf{S}} + \mathbf{\Phi}(\mathbf{b}+d\mathbf{b})) + (\mathbf{t}+d\mathbf{t}) \qquad (21)$$

6) Go back to step (2).

The above procedure is repeated until the change in **S** at the end of each iteration is less than a predetermined value.

III. RESULTS

Fig. 4 shows an example of segmenting tibia using the ASMs described in this paper. Fig. 4(a) is the original ultrasound image of a healthy volunteer's right leg. To produce the image, an ultrasound transducer rotates 360 degrees around the leg in a plane approximately 25 cm below the knee. A B-scan image is taken every 10 degrees. The 36 images are then combined to produce a compound image which is shown in Fig. 4(a). In the image, the boundary of tibia is vaguely visible. Fig. 4(b) shows an initial model shape which is manually placed over tibia area. Although the model shape shown in Fig. 4(b) appears as a continuous

contour, it is actually represented by 45 points, with the anchor point 1 facing the fibula bone. Fig. 4(c) shows the final model shape after 50 iterations. It can be seen that the final model shape matches the tibia boundary quite well.

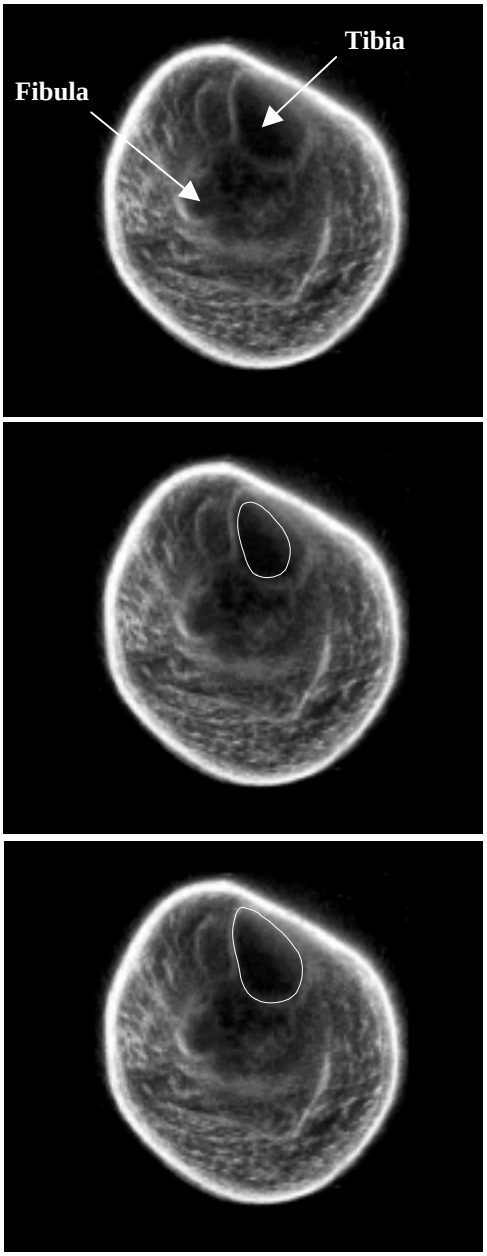

Fig. 4 An example of segmenting tibia from ultrasound image. (a) The original ultrasound image. (b) Initial model shape placed next to the expected tibia boundary. (c) Resultant model shape after 50 iterations.

IV. Discussion

The templates-based deformable models seem particularly suitable for segmenting tissue structures in medical ultrasound images. In such images, the boundaries of various organs (such as ventricles, bones, etc.) are often not clearly defined and sometimes are even incomplete. Techniques that heavily rely on local edges may produce a curve that strays far away from the true boundary of the targeted structure. The ASMs described in this paper uses a training set to generate a mean shape for tibia that is allowed to deform within a certain limit derived from the training set. As a result, the final result will unlikely stray far away from the true boundary.

The main difficulty in using ASMs seems to be in the stage of preparing the training set. For example, it is difficult to determine whether the training set contains just enough samples of the structure of interest. If a particular shape, which is not in the set, is significantly different from any samples in the set, then it will not be accurately segmented by the ASMs. On the other hand, if the number of samples in the training set is too large, manual generation of landmark points for each sample becomes very time-consuming. In our particular application, the shape of the cross section of tibia changes significantly from the proximal end to the distal end. A practical question then is whether to consider the entire tibia as one structure or to consider the proximal tibia as one structure and the distal tibia as another structure. Another consideration is to combine the cross section of distal tibia with that of fibula and treat the two contours as one structure. These are some topics of our future study.

ACKNOWLEDGMENTS

This project is partially funded by the National Institute on Disability and Rehabilitation Research, U.S. Department of Education.

REFERENCES

[1] P. He, K. Xue, Y. Wang, and Y. Fan, “A new strategy for 3D imaging of residual limbs using ultrasound.” *Proceedings* – 20th IEEE/EMBS Conference, pp. 2750-2753, 1998.

[2] T. Cootes, A. Hill, C. Taylor, and J. Haslam, “The use of active shape models for locating structures in medical images.” *Image and Vision Computing* 12(6):355-366, 1994.

[3] T. Cootes, C. Taylor, D. Cooper, and J. Haslam, “Training models of shape from sets of examples.” *Proceedings* – British Machine Vision Conference, Springer – Verlag, pp. 9-18, 1992.